Automation in Construction 93 (2018) 315–324

Contents lists available at ScienceDirect

Automation in Construction

journal homepage: www.elsevier.com/locate/autcon

EEG-based workers' stress recognition at construction sites

Houtan Jebelli[a], Sungjoo Hwang[b], SangHyun Lee[c,*]

[a] Tishman Construction Management Program, Department of Civil and Environmental Engineering, University of Michigan, 2350 Hayward St., Suite 1316 G.G. Brown Building, Ann Arbor, MI 48109, United States

[b] Department of Architectural and Urban Systems Engineering, Ewha Womans University, 52 Ewhayeodae-Gil, Seodaemun-Gu, Seoul 03760, Republic of Korea

[c] Tishman Construction Management Program, Department of Civil and Environmental Engineering, University of Michigan, 2350 Hayward St., Suite 2340 G.G. Brown Building, Ann Arbor, MI 48109, United States

ARTICLE INFO

Keywords:
Electroencephalogram (EEG)
Brain wave patterns
Construction workers' stress
Supervised learning
Workers' health, safety, and productivity
Wearable biosensors in construction sites

ABSTRACT

Taking into account that many construction workers suffer from excessive stress that adversely impacts their safety and health, early recognition of stress is an essential step toward stress management. In this regard, an electroencephalogram (EEG) has been widely applied to assess individuals' stress by analyzing brain waves in the clinical domains. With recent advancements in wearable EEG devices, EEG's ability can be extended to field workers, particularly by non-invasively assessing construction workers' stress. This study proposes a procedure to automatically recognize workers' stress in construction sites using EEG signals. Specifically, the authors collected construction field workers' EEG signals and preprocessed them to capture high-quality signals. Workers' salivary cortisol, a stress hormone, was also collected to label low or high-stress levels when they work at sites. Time and frequency domain features from EEG signals were calculated using fixed and sliding windowing approaches. Finally, the authors applied several supervised learning algorithms to recognize workers' stress while they are working at sites. The results showed that the fixed windowing approach and the Gaussian Support Vector Machine (SVM) yielded the highest classification accuracy of 80.32%, which is very promising given the similar accuracy of stress recognition in clinical domains where extricate and wired EEG devices were used and the subjects engage in minimal body movement. The results demonstrate that the proposed field stress recognition procedure can be used for the early detection of workers' stress, which can contribute to improving workers' safety, health, wellbeing, and productivity.

1. Introduction

Job stress has been defined as the negative physical and mental reactions to circumstances where job demands exceed workers' abilities. Construction is known as one of the most stressful occupations because of physically and psychologically demanding tasks performed in a hazardous work environment [1–4]. Workers' excessive occupational stress has been proven to increase the likelihood of errors, incidents, injuries, and health problems, and is linked to stagnant/declined productivity [5–8]. All of these issues are prevalent in the construction industry. Further, it was reported that 68% of construction workers suffer from excessive stress as a result of working in the construction industry [9].

To manage excessive occupational stress, recognizing workers' stress on site is an essential step. To date, considerable attention on individuals' electroencephalogram (EEG) signals has been paid to measure and monitor workers' mental status in the clinical domain. EEG is a noninvasive measurement of the brain's electrical activity, which is generated by firing neurons in the brain [10,11]. EEG thus represents central nervous system activities along the scalp [10–14]. The advantage of EEG in recognizing individuals' stress is in that it can quantify stress from brain wave patterns by overcoming the possible biases of survey-based psychological stress measurement methods [15]. Further, a recently available wireless and wearable EEG device can extend EEG's ability to non-intrusively assess the stress levels of construction field workers. If successfully applied in the field, continuous and affordable workers' stress recognition is enabled to overcome the limitations of other cumbersome methods in field applications, which may interfere with workers' ongoing work tasks (e.g., measuring the stress-related hormonal responses such as cortisol that require cumbersome hormone sample collection).

Recently, several research efforts have enhanced the applicability of EEG devices on the construction site [12,16–20]. For example, the authors' previous research proposed an advanced signal processing framework to acquire high-quality EEG signals from wearable EEG devices [21]. The use of this framework can overcome the major

* Corresponding author.
E-mail addresses: hjebelli@umich.edu (H. Jebelli), hwangsj@ewha.ac.kr (S. Hwang), shdpm@umich.edu (S. Lee).

https://doi.org/10.1016/j.autcon.2018.05.027
Received 5 January 2018; Received in revised form 22 April 2018; Accepted 20 May 2018
Available online 30 May 2018

limitations associated with applying wearable EEG devices to field workers, including considerable signal noises (i.e., artifacts). In addition, other research efforts also reinforced the potential for a few features (e.g., valence, arousal, and EEG power) extracted from EEG signals to capture different brain wave patterns while workers were subjected to different stressors [16,18]. The recognition of such patterns helps to understand workers' psychological states such as emotional states, attention levels, and mental workloads. Although these features can be used as informative signal features to understand the aforementioned psychological states, they are not enough when it comes to stress that is a very complex psychological state. In other words, an extensive range of EEG signal features is required to detect construction workers' stress due to complex EEG patterns from many different field stressors and among different subjects.

To address this issue, the objective of this paper is to develop a procedure to automatically recognize workers' stress, which uses a comprehensive set of EEG signal features from the EEG signals acquired at real construction sites from a wearable EEG device. This automatic stress recognition is particularly important to detect and manage workers' excessive stress on construction sites where workers' stress levels can vary significantly according to with numerous field stressors that change over time. To achieve this research objective, the authors firstly collected real construction workers' EEG signals using a wearable EEG device while they were working at real construction sites. Workers' salivary cortisol levels, known as a stress hormone, were measured to label the tasks as low or high-stress. After removing EEG signals artifacts, relevant time and frequency domain features in EEG signals were calculated by applying fixed length and sliding windowing approaches. Then, several supervised learning algorithms were applied to select the best classifier to recognize worker's stress. Finally, by comparing the developed field stress recognition procedure with ones used in the clinical domains, the applicability of the developed procedure for construction workers' stress recognition will be demonstrated.

2. Stress and EEG

Despite different stress definitions, there is an area of agreement among these definitions; stress is the nonspecific reaction of the body and mind to changes in demands that affect human nervous system [22]. Stress interrupts the normal function of the human nervous system. The brain reacts to these distortions by releasing a series of chemical reaction (i.e., stress hormones) such as cortisol to retain the normal activity of nervous systems. Particularly, a change of currents during activation of the brain caused by stress produces a magnetic field, and this magnetic field over the scalp is measurable using EEG. Because EEG signals can provide rich information about individuals' mental status related stress, many attempts have been made to recognize and measure subjects' stress using EEG signals, mostly in the clinical domain. For instance, researchers in [23] showed the capability of EEG in differentiating different levels of arousal, which is defined as the state of being awoken and the degree of attention and closely associated with stress by changing under different stressors [24]. Applied an audio and cognitive stimulus to recognize emotions related to stress (e.g., sadness, anger, and surprise) by applying a machine learning algorithm using subjects' EEG signals. They reported a prediction accuracy as good as 61.8%. The researchers in [25] calculated six EEG features to classify five different emotions including stress and applied a Support Vector Machine (SVM), which resulted in the recognition rate of 41.7%. The authors in [13] used the induction visual images to generate two different levels of stress in a controlled environment such as calm-neutral and negatively-excited and obtained the accuracy of 78.3% using EEG signals with SVM classifier. The researchers in [26] reported the stress recognition accuracy of 83.33% using individuals' EEG signals. They applied a SVM to recognize the stressed subjects in a shelter center. The authors in [14,27] recognized individuals' stress while they induced mental stress by the Stroop color-word. They reported the prediction accuracies of 75% and 85.71%, respectively.

However, these research efforts have not been applied in the field. If applied using newly available wearable EEG devices, such stress recognition accuracies would not be guaranteed because of several hurdles in field application. These hurdles include low EEG signal quality caused by not only signal artifacts from workers' movements but also the poor spatial resolution (i.e., wearable EEG devices normally have 7–16 electrodes compared to 32–256 electrodes placed in wired EEG devices used in the clinical domain) and the low temporal resolution (i.e., wearable EEG devices data recording rate is in the range of 128–500 Hz compared to 2–100 kHz data recording range for the wired EEG devices used in the clinical domain) of wearable EEG devices. In addition, many stressors affecting stress in the real work environment requires the use of a more extensive range of signal features to recognize stress. All these challenges should be resolved before EEG signals are used to recognize construction workers' field stress.

3. EEG-based field stress recognition procedure

3.1. Overview

Fig. 1 represents an overview of an EEG-based field stress recognition procedure developed in this study. It aims to achieve a similar accuracy of stress recognition in clinical domains overcoming all the hurdles discussed earlier. As the first step, EEG signals across 14 different channels were collected using an off-the-shelf wearable EEG device. Workers' EEG signals were labeled based on their stress-related hormone (A in Fig. 1). Then, EEG signal artifacts were removed by applying an EEG signal processing framework signals suggested by the authors' previous work [21] (B in Fig. 1). After removing signal artifacts, EEG features in time and frequency domain were extracted (C in Fig. 1). Features with the highest distinguishing power were selected among a comprehensive list of EEG features selected from the literature. Then, to select the best classifier to recognize workers' stress, the performance of several supervised learning algorithms were evaluated to recognize workers' stress (D in Fig. 1). Details on each step will be described in the following sub-sections.

3.2. EEG preprocessing and artifacts removal

Although the EEG device is designed to record brain activity, it also records electrical activity arising from other sources than the brain [28]. As mentioned in Section 2, EEG signals contain a significant amount of extrinsic and intrinsic artifacts, which obscure the brain waves. The signal artifacts are significantly greater when acquiring EEG signals from construction workers at actual construction sites, due to workers' extensive movements and existing different environmental factors (e.g., construction equipment's noise). To solve this issue, the authors previously proposed and validated a signal processing framework suggested [21] to remove EEG signal artifacts thereby acquiring high-quality EEG signals at construction sites.

Below is a summary of artificial removal steps in this framework, and more information can be found in [21]. Usually, extrinsic artifacts (e.g., electrode popping, movement artifacts, environmental noise, and wiring noise in the EEG sensor) have different frequencies with brain waves. Therefore, filtering the frequencies out of the range of EEG signals will remove most of the extrinsic artifacts. A bandpass filter with a higher cutoff frequency of 64 Hz and a lower cutoff of 0.5 Hz was used to remove most of the present extrinsic artifacts that cause slow and rapid changes in the EEG signals. The lower cutoff frequency criterion to design the band pass filter was based on the frequency range of the rhythmic brain potentials detected with surface electrodes placed on the head (e.g., Delta waves 0.5–4 Hz, Theta waves 4–7.5 Hz, Alpha waves 7.5–13 Hz, Low beta waves 13–15 Hz, Beta waves 15–20 Hz, High beta waves 20–38 Hz, and Gamma waves 38–higher Hz) and the higher cutoff frequency was selected considering the EEG data

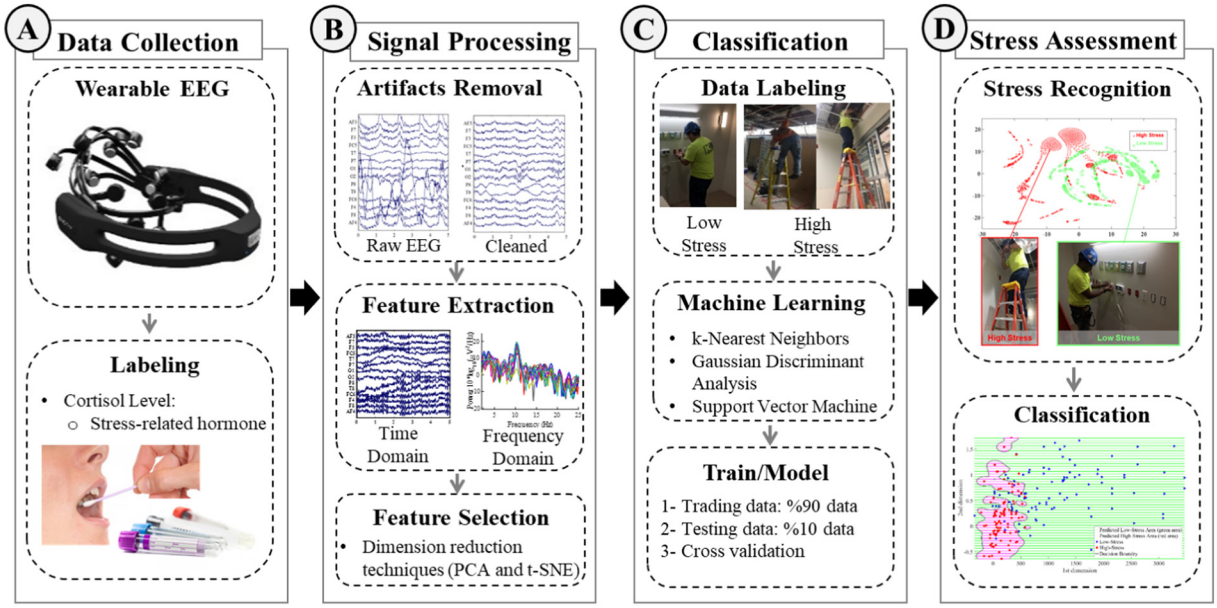

Fig. 1. An overview of field stress recognition procedure.

recording rate (128 Hz) and Nyquist frequency, which is the highest frequency that we can expect to be present in the sampled data considering the recording rate. Nyquist frequency is equal to the half of the sampling rate (64 Hz in this paper). Also, a notch filter, which filters out a very narrow band of frequencies from a signal [29], was used to remove the ambient electrodes' wire noise that comes from the power line interference signal (e.g., 60 Hz). Unlike extrinsic signal artifacts, intrinsic signal artifacts are within the same frequency range as the EEG signals. To eliminate intrinsic artifacts, an independent component analysis (ICA) was applied to detect the artifactual components (e.g., eye movement, blinking, and muscle artifacts) existing in EEG recording signals [21]. ICA method can isolate EEG intrinsic artifacts from the original EEG without losing EEG signal [30] by identifying the artifactual EEG components in the EEG and subtracting the components that are associated to intrinsic artifacts to achieve a clean EEG signal. ICA method has been commonly used in EEG research in the clinical domain to detect and remove intrinsic EEG artifacts [31–35]. More detailed explanations about the pattern of artifactual components recorded by a wearable EEG device at actual construction sites is provided by authors' previous work [21].

3.3. EEG signals feature extraction and selection

The next step is to select useful features that can be used to recognize stress. In most of the machine learning algorithms, selection of relevant features is of critical importance because it affects not only the accuracy of classification but also the computational cost of classification algorithms. A feature is an informative and measurable property of the detected signals. According to the literature, there are two well-known feature selection methods: a correlation-based method and a wrapper method [36,37]. Correlation-based methods select the most useful features by ranking them with correlation coefficients. Wrapper methods assess subsets of features according to their usefulness to a given predictor [38]. Wrapper methods make various subsets of features and run learning algorithms, and the feature subsets that provide the best accuracy will be considered as the relevant features. Wrapper methods are not very practical to be used on a large number of features due to high computational cost. When dealing with EEG signals, there are a large number of features both in time and frequency domains. Learning on all the possible subsets combination and comparing the accuracy requires a high computational cost and time. Unlike wrapper methods, correlation-based methods filter out the features that have the least effect on the classification. So in this paper, the authors firstly applied the correlation-based method to filter out the features with least correlation to the prediction accuracy. Then, the authors examined the optimal feature subsets that maximize classification accuracy by applying a wrapper method. 540 features were derived from 14 EEG channels (40 features for each EEG channel) from the existing literature in time and frequency domains. Among all those features, 224 features were selected using correlation-based methods. Considering the overall prediction accuracy and computational cost and time, the top 80 features (Table 1) that resulted in the greatest prediction accuracies were selected after applying a wrapper based methods on the selected 224 features.

Calculation of a feature over one single EEG reading is not informative, since EEG signals were recorded at 128 Hz, thus the number of data points is large (128 data points per second). To overcome this problem, features will be extracted from blocks of continuous readings referred to as windows. Previous researchers found that the window size between 3 and 12 s is an effective window size while classifying individuals' mental status using EEG signals [39]. To find the optimal window size to recognize workers' stress, the window sizes of 1 to 12 s increased by 1-s step were tested respectively. The window size of 5 s was determined as the optimal window size that leads to the best recognition performance.

One method of partitioning the data into different windows is to define a single continuous segment that spans an entire action sequence data (i.e., fixed windowing approach). Features are then extracted from these windowed segments and used in a machine learning algorithm to classify a fixed length testing segment. This ensures that an entire action sequence is captured in each feature used for training (A in Fig. 2). An alternative windowing approach to a fixed one is to segment data using a sliding window approach (B in Fig. 2). Therefore, to select the best windowing approach, the proposed procedure will test both of these windowing methods and select the one with highest classification accuracy.

3.4. EEG classification

In this paper, different supervised machine learning algorithms are thoroughly tested using fixed and sliding windowing approaches. The tested algorithms included *k*-Nearest Neighbors (*k*-NN), Gaussian

Table 1
Time and frequency domains features, extracted from EEG signals.

	Features	Equation	Explanation
Time domain	Cumulative maximum	$Cmax_{ij} = \max(EEG_{1:i,\ j})$	Maximum amplitude of channel j up to sample i
	Cumulative minimum	$Cmax_{ij} = \min(EEG_{1:i,\ j})$	Minimum amplitude of channel j up to sample i
	Mean value	$\mathrm{MAV}_j = \frac{\sum_{i=1}^{N} EEG_{ij}}{N}$	Average absolute value of amplitude among different channels
	Median value	$Med_j = sort(EEG)_{\frac{N+1}{2},j}$	Median of the signal among different EEG channels
	Smallest window elements	$Min_j = \min_i EEG_{ij}$	Minimum amplitude among different channels
	Moving median with window size k	$MovMed_{i,\ j} = Median(EEG_{i:i+k-1,\ j})$	Median of the signal of channel j in a widow with size k samples
	Maximum-to-minimum difference	$MaxMin_j = \max_i EEG_{ij} - \min_i EEG_{ij}$	Difference between maximum and minimum of the EEG signals amplitude among different EEG channels
	Root-mean-square level	$\mathrm{RMS}_j = \sqrt{\frac{\sum_{i=1}^{N} EEG_{ij}^2}{N}}$	Norm 2 of the EEG signals divided by the square root of the number of samples among different EEG channels
	Peak-magnitude-to-RMS ratio	$\mathrm{PRMS}_j = \frac{\|\| EEG_{:,j} \|\|_\infty}{\sqrt{\frac{\sum_{i=1}^{N} \| EEG_{ij} \|^2}{N}}}$	Maximum of the EEG signal amplitude divided by the RMS_j
	Root-sum-of-squares level	$\mathrm{RSS}_j = \sqrt{\sum_{i=1}^{N} \|EEG_{ij}\|^2}$	Norm of the EEG signals among different channels in each window
	Standard deviation	$\mathrm{STD}_j = \sqrt{\frac{1}{N-1}\sum_{i=1}^{N} EEG_{ij}^2}$	Deviation of EEG signals among different channels in each window
	Variance	$\mathrm{VAR}_j = \frac{1}{N-1}\sum_{i=1}^{N} EEG_{ij}^2$	Variance of the signal EEG amplitude among different channels
	Peak	$Pk_j = \max_i EEG_{i,j}$	Maximum value of EEG amplitude among different channels in time domain
	Peak location	$LPk_j = \underset{i}{\mathrm{argmax}}\, EEG_{i,j}$	Location of maximum EEG amplitude among channels
	Peak to Peak	$PP_j = LPk_j - \arg\max_{i, i \neq LPk_j} EEG_{i,j}$	Time between EEG signal peaks between the various windows
	Kurtosis	$k_j = \frac{\frac{1}{N}\sum_i (EEG_{ij} - \mathrm{MAV}_j)^4}{\left(\frac{1}{N}\sum_i (EEG_{ij} - \mathrm{MAV}_j)^2\right)^2}$	Shows the sharpness of EEG signals peak
	Total zero cross number	$ZCN_j = \|\{i \mid EEG_{i,\ j} = 0\}\|$	Number of points where the sign of EEG amplitude changes
Frequency Domain	Alpha mean power	$\alpha_j = power(EEG_{:,\ j}, f \in [8Hz, 15Hz])$	Power of the EEG signal in channel j in frequency domain in the interval $[[8Hz, 15Hz]]$
	Beta mean power	$\beta_j = power(EEG_{:,\ j}, f \in [16Hz, 31Hz])$	Power of the signal in Beta interval
	Delta mean power	$\delta_j = power(EEG_{:,\ j}, f \in [0Hz, 4Hz])$	Power of the signal in Delta interval
	Theta mean power	$\theta_j = power(EEG_{:,\ j}, f \in [4Hz, 7Hz])$	Power of the signal in Theta interval
	Valence	$V = \frac{\alpha(F4)}{\beta(F4)} - \frac{\alpha(F3)}{\beta(F3)}$	Level of happiness
	Arousal	$A = \frac{\alpha(AF3 + AF4 + F3 + F4)}{\beta(AF3 + AF4 + F3 + F4)}$	Level of excitement
	Median frequency	$power(EEG_{:,\ j}, f \in [0Hz, MEDF_j]) = power(EEG_{:,\ j}, f \in [MEDF_j, 64Hz])$	Half of the signal power of channel j is distributed in the frequencies less than $MEDF_j$

Discriminant Analysis (GDA), Support Vector Machine (SVM) with different similarity functions (linear, Gaussian, cubic, and quadratic). Additionally, the authors explored the Hidden Markov Models (HMM), decision tree, and Logistic Regression approaches for classification. However, their preliminary results were discouragingly lackluster and were not pursued further. 10-fold cross validation was utilized for the selected classifiers to validate obtained classification accuracies; classification was performed ten times using 90% of data for training and 10% of data for testing each time.

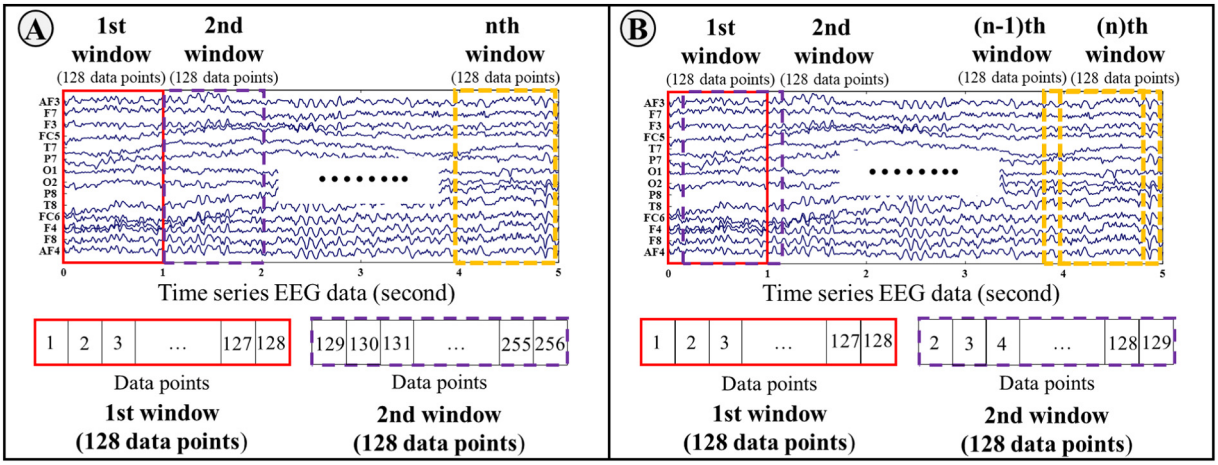

Fig. 2. EEG windowing approaches: (a) fixed windowing approach; (b) sliding windowing approach.

3.5. k-NN classification

k-NN is a memory-based algorithm, which utilizes the entire database for prediction, based on a similarity measure in the instance space [40]. Memory-based algorithms find a set of nearby data points in the instance space with similar features, known as neighbors [41]. To predict the label of a new data point, a group of nearby neighbors referred to as the neighborhood is formed. *k*-NN is based on the assumption that the nearby data points in the instance space have the same class [42].

When a new unlabeled data $X_i \in R^d$ arrives, *k*-NN measures the distance, $d_E(X_i, Z_j)$, between the unlabeled target data points $\{X_1, X_2, X_3, \ldots, X_m\}$, $i = 1, 2, \ldots, m$ and labeled training data points $\{Z_1, Z_2, Z_3, \ldots, Z_n\}$, $j = 1, 2, \ldots, n$. Where n is the size of training data set and m is the number of unlabeled data points.

$$d_E(X_i, Z_j) = \|X_i - Z_j\|_2 = \sqrt{\left(\sum_{l=1}^{d} (x_i^l - z_j^l)^2\right)} \tag{1}$$

After calculating the distance between unlabeled data points and training data points, the subset of k nearest neighbors to the unlabeled data point is defined as $\theta_k(X_i)$ where $\theta_k(X_i) = \{\theta_1, \theta_2, \theta_3, \ldots, \theta_k\} \subseteq \{Z_1, Z_2, Z_3, \ldots, Z_n\}$ and the class label for θ_l, l = 1,2,3,…,k defined as $L(\theta_l)$ and is derived from Eq. (2).

$$L(\theta_l) = y \text{ where } y \in \{+1\,(\textit{high stress}), -1(\textit{low stress})\} \tag{2}$$

Finally, the predicted label for X_i is defined as the majority labels of $\theta_k(X_i)$ using Eq. (3).

$$L(X_i) = \begin{cases} +1 \textit{ high stress if } |A_{+1}| \geq |A_{-1}| \\ -1 \textit{ low stress if } |A_{+1}| < |A_{-1}| \end{cases} \tag{3}$$

where A_{+1} is the set of the neighbor data points labeled as $+1$ (high stress), and A_{-1} is set of the neighbor data points labeled as -1 (low stress).

In this research, the performance of *k*-NN algorithm was optimized by selecting the smallest k ($k = 100$) given the highest prediction accuracy. Euclidean distance metric was chosen to measure the distance between unlabeled target data points X_i and labeled training data points Z_j.

3.6. GDA classification

GDA is a generative machine learning method that predicts the unlabeled data by modeling a Bernoulli probability for two classes of data (-1 indicating low stress and $+1$ shows high stress) using Eqs. (4) and (5).

$$P(x|y = -1) = N(\mu_{-1}, \Sigma) = \frac{1}{(2\pi)^{\frac{n}{2}}(|\Sigma|)^{\frac{1}{2}}} \exp\left(\frac{1}{2}(x - \mu_{-1})^T \Sigma^{-1}(x - \mu_{-1})\right) \tag{4}$$

$$P(x|y = +1) = N(\mu_{+1}, \Sigma) = \frac{1}{(2\pi)^{\frac{n}{2}}(|\Sigma|)^{\frac{1}{2}}} \exp\left(\frac{1}{2}(x - \mu_{+1})^T \Sigma^{-1}(x - \mu_{+1})\right) \tag{5}$$

where x_i is training data points and y_i is the labels, μ_{-1} *and* μ_{+1} are different classes mean values, and Σ is the covariance of $N(\mu, \Sigma)$.

GDA expresses the joint likelihood of a set of data $i = 1, 2, \ldots, n$ using Eq. (6).

$$l(\phi, \mu_{-1}, \mu_{+1}, \Sigma) = \prod_{i=1}^{n} P(x_i, y_i) = \prod_{i=1}^{n} P(x_i|y_i) P(y_i) \tag{6}$$

where x_i is the features for *i*th data point and y_i represents data point class and $\phi = \frac{\sum_{i=1}^{n} y_i}{n}$ is the parameter of Bernoulli distribution.

Finally, the predicted label for X_i defined as the maximize conditional probability of labels given data point x using Eq. (7).

$$L(X_i) = argmax_{k=1,\ldots,m} P\left(y\ |x\right) = argmax\left(\frac{P(x\ |y)p(y)}{p(x)}\right)$$
$$= argmax\left(P(x\ |y)p(y)\right)$$
$$= = \begin{cases} +1 \textit{ high stress if } P(y = 1\ |x) > P(y = -1\ |x) \\ -1 \textit{ low stress if } P(y = 1\ |x) < P(y = -1\ |x) \end{cases} \tag{7}$$

3.7. SVM classification

SVM is a supervised learning method frequently used in machine learning and data mining [43]. SVM has been introduced as an appropriate classifier for physiology data class actions [44]. SVM creates hyperplanes that separate data points of a binary classification problem. SVM applies an iterative learning process to converge into an optimal hyperplane that maximizes the margin between data points of two classes by minimizing following objective function.

$$\min_{w,b,\xi} \frac{1}{2}\ ||w||^2 + \frac{C}{n}\sum_i^n\ \xi_i\ \ for\ i = 1,\ \ldots,N \tag{8}$$

where $C > 0$ is a user specified tuning parameter, and n is the number of training data points.

In linear SVM, the separating hyperplane $\mathscr{H}$ is defined as $\mathscr{H} = W^T X = \{x\ |<w, x> + b = 0\}$ where w is a normal vector and $w \in R^m$, $b \in R$ and $<.,.>$ denoting the inner product. Linear-SVM solve the objective function (Eq. (8)) by considering following constrains $[y_i(<w, x> + b) \geq 1 - \xi_i, i = 1, \ldots, n, \xi_i \geq 0]$.

If the data points are not separable using linear SVM, a non-linear SVM employs a transfer function $\phi(X)$, which maps the data point x_i of data space to a feature space H where the separable hyperplane can be defined. Non linear-SVM uses a mapping function $\phi(X)$ to create a *m*-dimensional feature space from a *n*-dimensional input data, in which m is greater than n. In other words, SVM maps data into a richer feature space, which allows for a definition of the hyperplane that separates the data points that are not easily separable in the input data dimension. Non-linear SVM solves the objective function (Eq. (8)) by considering the following constraints $[\text{s.t} y_i\left(\sum_{j=1}^{m} w_i \phi_j(X_i) + w_0\right) \geq 1 - \xi_i,\ \ i = 1,\ \ldots,n,\ \ \xi_i \geq 0]$, where y_i represent class labels, w is the weigh vector, $\phi(X_i)$ is the mapping function, ξ_i is a nonnegative slack variable that generalized the classifier with soft margins, w_0 is constant that captures offset of data points, and N is training data points number.

In this paper, the authors examine both linear and non-linear SVMs. Three different mapping functions, including cubic polynomial: $K(x_i, x_j) = (1 + x_i^T x_j)^3$, quadratic polynomial: $K(x_i, x_j) = (1 + x_i^T x_j)^4$, and Gaussian radial basis function: $K(x_i, x_j) = \exp\left(\frac{-\|x_i - x_i\|^2}{2\sigma^2}\right)$, were selected for non-linear SVM. After determining $\mathscr{H}$ using Eq. (8) by selecting appropriate mapping function, unlabeled data class will be decided using decision function.

$$L(x_i) = sign\ (W^T \phi(x_i)) = \begin{cases} +1 \textit{ high stress} \\ -1 \textit{ low stress} \end{cases} \tag{9}$$

4. Field construction workers' EEG data acquisition

To examine the performance of the developed field stress recognition procedure, the authors collected EEG signals from three real construction sites: an office building renovation site in Detroit, Michigan (collected on March 18–25, 2016); a hospital renovation site in Gary, Indiana (obtained on February 22, 2017); and one off-site HVAC-sheet metal fabrication shop in Wixom, Michigan (collected on March 28–April 4, 2016) using an off-the-shelf wearable EEG device. The data collection protocol was approved by the University of Michigan Institutional Review Board (IRB Approval no. HUM00102068).

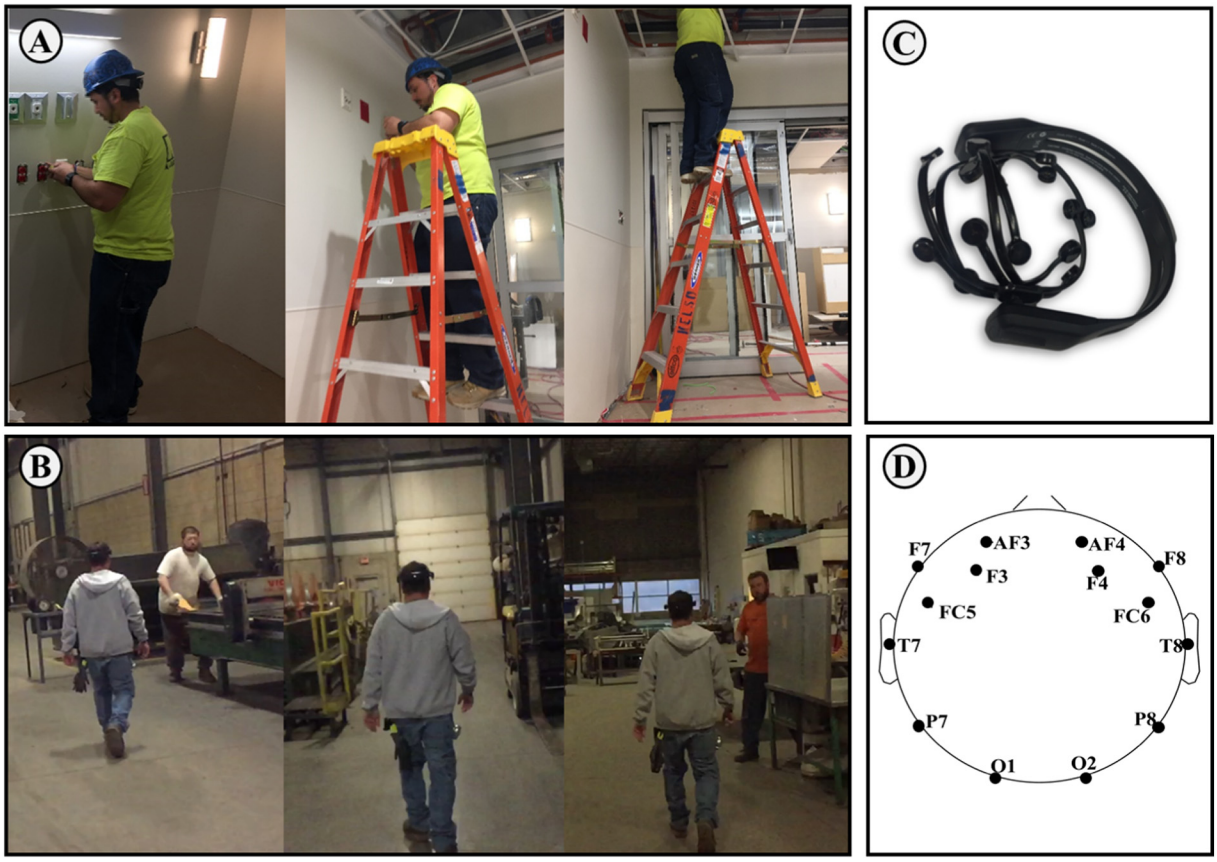

Fig. 3. EEG data collection in-field; (a) working in a construction site with different work conditions; (b) working in an off-site shop while subjects work different amounts of working hours; (c) wearable EEG headset (Emotiv EPOC+); (d) location of EEG electrodes.

4.1. Subjects and data acquisition process

EEG signals were obtained from 11 male workers. Subjects reported no history of epilepsy, learning disabilities, and mental disorders. Seven subjects working at on-site construction sites were asked to perform the same repetitive tasks in three different conditions with varying levels of operating hazards (i.e., working on the ground, at the top of a ladder, and in a confined space), as shown in A of Fig. 3. Four subjects working in an off-site fabrication shop were asked to perform their daily tasks at different times with a varied number of working hours after resting (i.e., right after, and one or two hours after the scheduled resting time), which could yield different stress levels, as shown in B of Fig. 3. The authors' previous study showed that workers feel more negative emotions while working at the top of a ladder/in a confined space and continuous working without taking an enough break than working on the ground and working after having enough break time [45].

Using an off-the-shelf wearable EEG device (e.g., Emotiv EPOC+ that this study used as denoted by C in Fig. 3), workers' brain waves from 14 channels (D in Fig. 3) were captured. Data was with a rate of 128 Hz deliverable. The data-collecting resolution was set at 14 bits with the connectivity at a 2.4 GHz band and a dynamic range of 8400 μV (pp). Data collection was approved by the University of Michigan's Institutional Review Board. Before starting the data collection sessions, subjects were informed of the purpose of this study and provided with a comprehensive explanation of the data collection process.

4.2. Data labeling

In order to select the appropriate labels for data (i.e., low stress and high stress), the authors selected two job site stressors: working hazards and tiredness. Working in hazardous conditions (e.g., working at the top of a ladder and working in a confined space) and feelings of tiredness over time (e.g., continuous work without taking a break time) adversely affects workers' stress levels [46–48]. These tasks were labeled as the tasks with higher-level stress. On the other hand, working on the ground level and working right after taking a short break time were labeled as low stress tasks.

In addition to these assumptions, the authors screened subjects' stress by measuring their cortisol levels to confirm these assumptions. To screen the data and select the most appropriate datasets to train and test the field stress recognition procedure, the authors measured subjects' cortisol levels obtained from their saliva samples after each session. A higher cortisol level indicates a higher stress level [49]. Out of 11 subjects, we selected 7 who had significantly higher cortisol levels while working in hazardous conditions and working in a row without resting. Table 2 shows demographic characteristics of the selected seven subjects. Table 3 summarized the cortisol level, data size, and assigned labels to different datasets. One notable point is that there is not a significant change in the cortisol level of Subject 2, who works in a shop, while working right after the rest (cortisol level is 0.08 μg/dL) and 1 h after the rest (cortisol level is 0.10 μg/dL). However, this subject asked to stop the experiment because of the high occupational

Table 2
Subjects sample information (n = 7).

Statistical parameters	Age (years)	Height (ft.-in.)	Weight (lb)	Working experience (years)
Mean	37.9	5 10	202.3	16.4
SD	8.8	0 4	30.4	9.8
Min value	26.0	5 3	151.0	3.0
Max value	50.0	6 3	235.0	31.0

Table 3
Overview of participants' data size, cortisol level, and label.

Site	Subject	Session#	Work conditions	Cortisol [μg/dL] (%CV*)	Data size [128 data/s]	Label
On-site	1	1	At ground	0.21 (8.00%)	76,800	Low stress
		2	At the top of a ladder and in confined space	0.4 (7.48%)	76,800	High stress
	2	1	At ground	0.16 (2.77%)	76,800	Low stress
		2	At the top of a ladder and in confined space	0.36 (4.12%)	76,800	High stress
	3	1	At ground	0.10 (10.81%)	76,800	Low stress
		2	At the top of a ladder and in confined space	0.16 (10.28%)	76,800	High stress
Off-site (Shop)	1	1	Right after rest	0.30 (1.72%)	61,440	Low stress
		2	1 h after rest	0.40 (3.32%)	61,440	High stress
	2	1	Right after rest	0.08 (11.09%)	61,440	Low stress
		2	1 h after rest	0.10 (5.59%)	61,440	High stress
	3	1	Right after rest	0.11 (0.96%)	61,440	Low stress
		2	2 h after rest	0.28 (7.30%)	61,440	High stress
	4	1	Right after rest	0.39 (0.93%)	61,440	Low stress
		2	2 h after rest	0.67 (2.05%)	61,440	High stress

Note: *CV = Percentage coefficient of variation of cortisol levels, CV lower than 15% is known as a reliable cortisol measurement.

stress this subject perceived after 1 h of the break time, so that we assigned a high stress label for this data.

5. Results

The authors applied the proposed field stress recognition procedure on the data collected from real construction sites after randomly dividing 90% of the data into training and 10% into testing data. Table 4 shows the classification accuracies among all the tested methods based on the fixed and sliding window approaches. The classification accuracies were calculated as the proportion of the correctly predicted results (both true high stress and low stress) among the total number of the tested data point. Gaussian SVM, which used the fixed window approach to extract the features as learning inputs, showed the highest prediction accuracy of 80.32% among the tested supervised learning methods.

A comparison of different windowing methods revealed that fixed window size showed better prediction accuracy among all the classification algorithms. Visualization of the trained SVMs provides us with intuition about the classification's performance. Fig. 4 visualizes the decision boundaries and the performance of various classification methods of a randomly selected subset of data after applying a dimension reduction algorithm (principal component analysis method (PCA)) to reduce the dimensions of the feature vector to two dimensions. The first PCA component captures the highest amount of the variance in the feature vector. The second PCA component is orthogonal to the first principal component to capture the variance in the feature vector that is not captured by the first principal component. We normalized all the features before applying the PCA. Therefore, the results are all dimensionless. In Fig. 4, the light-gray background shows the area that is predicted by the classifier to be low-stress and the dark-gray background shows the area predicted to be high-stress. Gray triangle and white circle points show the actual labels of the data points. As shown in Fig. 4, Gaussian SVM shows the best distinction between low and high stress datapoints and better prediction performance compared with other algorithms.

Table 4
Classification accuracies of each tested algorithm.

Algorithm	Classification accuracy (%)	
	Fixed window	Sliding window
k-NN	65.80	61.12
GDA	74.92	69.98
Linear SVM	75.9	69.54
Cubic SVM	77.71	65.25
Quadratic SVM	69.62	63.24
Gaussian SVM	80.32	72.15

6. Discussion

The results show the capability of the proposed procedure in field recognition of construction workers' stress while working at real construction sites using EEG signals recorded from a wearable EEG device. The results of the proposed procedure are competitive with other stress recognition algorithms with a binary labeling setting in the clinical domain that are using a wired-EEG device in the controlled environment while their subjects were in stationary conditions with the minimal body movements: 85.60% in [50]; 87.30% in [51]; 80.43% in [52]; and 77.90% in [53]. For instance, the researchers in [51] recorded the brain waves of 12 healthy male subjects using an exquisite and wired EEG device. They recognized subjects' stress while subjects were under the stress of solving arithmetic problems. Subjects were asked to minimize their head movement during the data collection to minimize EEG signal artifacts. They reached the average classification accuracy of 87.30% by applying a SVM. Compared with the existing stress recognition procedures, the proposed stress recognition in this research provides a promising result considering that acquiring and processing the EEG signal was challenging from significantly moving subjects during the field data collection using a wearable EEG.

Among all tested classifiers used in the field stress recognition procedure, SVM showed higher prediction accuracy; this can be related to the high performance of SVM to deal with overfitting by tolerating some misclassifications on the training dataset. In recognizing stress using EEG signals, due to the number of EEG channels and the complexity of EEG signals, the authors need to have a large number of features to recognize stress appropriately. As such, the increasing number of features increases the probability of overfitting in training process. SVMs algorithms tend to be resistant to the overfitting problem. This is because SVM is optimizing its parameters over the training process to prevent the overfitting problem [54]. To decrease the probability of overfitting, SVM derives a generalization error bound, which depends on the SVM margin and is independent of the outliers and the dimensionality of feature space. As a result, it is expected that SVM will demonstrate reliability when dealing with large dimensions feature space data such as EEG signals.

Conversely, *k*-NN showed the lowest prediction accuracy among all the selected methods; this might be related to the inductive bias of *k*-NN method. *k*-NN inductive bias corresponds to the underlying assumption of *k*-NN method that classifies each instance data point *i* as the class label of the majority of other *k* neighboring instances by measuring Euclidean distance. This causes a practical problem while dealing with EEG signals that require measuring a large number of signal features among different channels to represent signals patterns adequately. *k*-

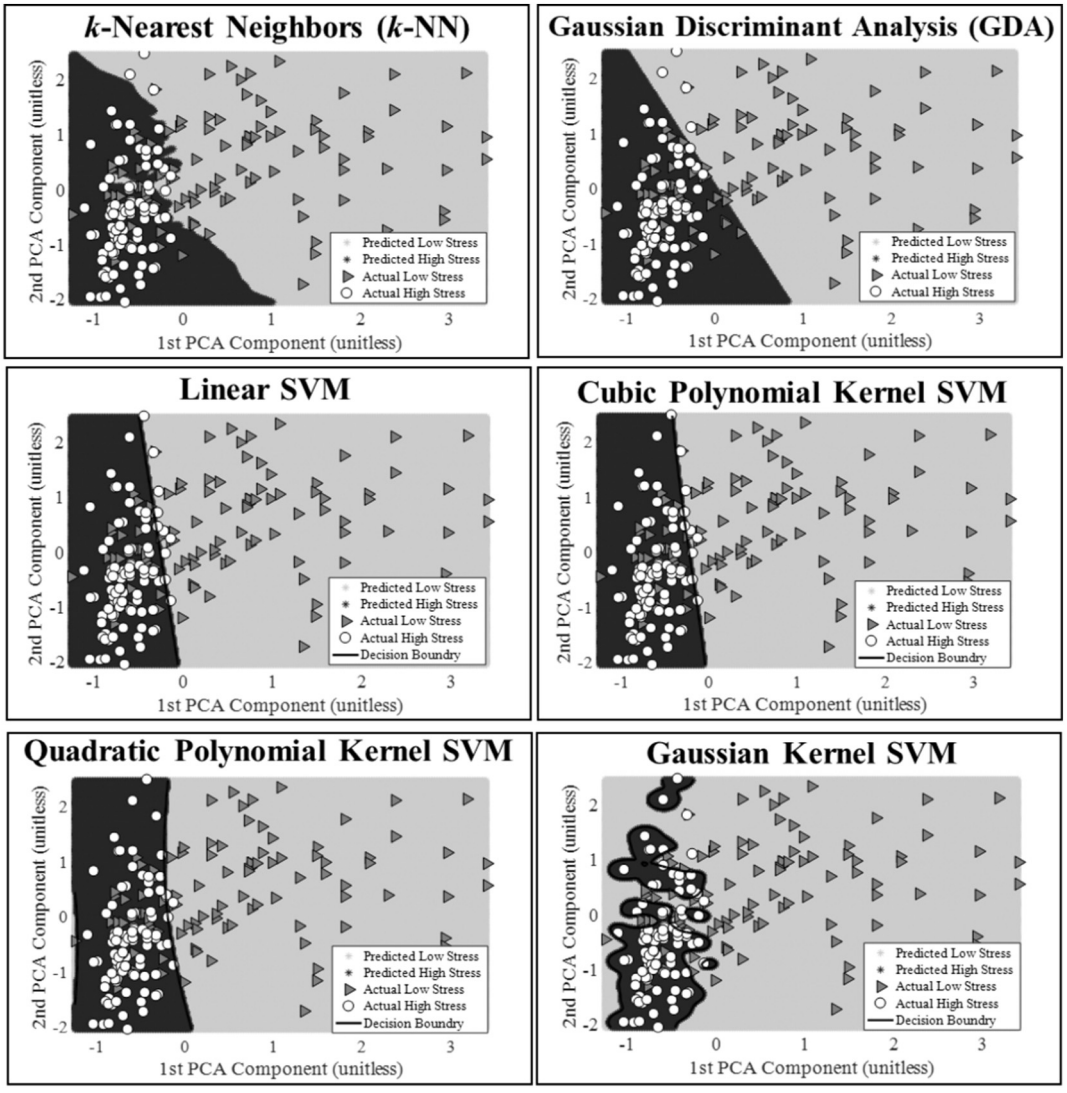

Fig. 4. Hyperplanes and decision boundaries by applying different classifications.

NN algorithm measures the distance between instances based on all features of the instance and considers the same weight for all the features; this becomes problematic for some data windows that only a small subset of the entire feature set is the discriminative features. Also, the *k*-NN performance is sensitive to noisy features. Although we removed a large number of signal artifacts, however, it is not possible to remove all the artifacts from EEG recording and EEG signals usually known as noisy signals, and there are some sources of noise that are unavoidable.

Upon further investigation of the misclassified labels, the authors noticed that 71% of the misplaced labels occurred among low-stress level detection. In other words, the classification accuracy is consistently better for high-stress detection rather than low-stress detection. This can be explained by the better performance of selected stressors to elicit high stress (e.g., working at the top of a ladder in a confined space) comparing with the stressor that has been chosen to cause low-stress conditions (e.g., working on the ground).

One unanticipated finding was that the applying sliding windowing method to extract EEG features led to a lower stress recognition prediction accuracy compared to fixed windowing approach among all the selected method. Applying the sliding windowing approach to extract EEG features increases the size of the training set and may smooth specific features, as well as provide consistent feature mapping inputs between training and testing steps. On the other hand, it may increase the computational cost and time as well as decrease the testing accuracy as the results of overfitting during the training process. Also, considering that sequential EEG signals have different levels, applying this technique will increase the likelihood of mislabeling EEG signals.

Several limitations still exist and need to be addressed in the future research. Different subjects show different brain wave patterns while facing the same stressors. These various patterns among different subjects adversely affect the performance of the proposed stress recognition procedure due to the static nature of the supervised learning algorithms used in the proposed procedure. To further improve the stress recognition accuracy, the authors suggest applying multi-subjects/tasks learning algorithms, which optimize classifier parameters for different tasks and subjects.

In addition, the recognition of varying stress levels will help to enhance the suggested procedure in this research. Although the Gaussian SVM classifier proposed in this research separated data into two classes (low stress and high stress), recognition of more classes can be done in future research by plugging in voting algorithms to the proposed procedure in this research [55].

7. Conclusions

This study developed and examined a field procedure to recognize construction worker's stress at real construction sites by applying

supervised learning algorithms stress using a broad range of EEG signal features. To select the best classifier in this procedure, this study examined the performance of several supervised learning algorithms in recognizing worker's stress from EEG signals collected at the real construction site using an off-the-shelf wearable EEG device. Notably, based on the results garnered from seven workers and among all tested classifiers, Gaussian SVM, which relies on a fixed windowing approach has the highest stress recognition accuracy. This accuracy of recognizing field workers' stress level in a real construction site is very promising given the competitive accuracy of stress recognition in clinical domains where extricate and wired EEG devices were used and stressors were controlled in a laboratory setting. The proposed field stress recognition procedure can be used as a mean toward affordable and continuous monitoring of workers stress under various stressors in construction sites, which can contribute to workers' stress management. It is noteworthy to mention that despite the large size of datasets (952,320 datapoints in total) and applying a validation step (10-fold cross-validation), the data was collected from seven subjects. To confirm the performance of the proposed framework in recognizing the stress level of workers with various trades, it is recommended that future studies further examine the performance of the proposed framework using a bigger sample size collected from more workers.

Acknowledgment

The authors would like to acknowledge their industry partners for their help in data collection, as well as anonymous participants who participated in the data collection.

References

[1] M. Jones, M. Saad, Managing Innovation in Construction, Thomas Telford Ltd, London, UK, 2003 (ISBN: 978- 0727730022).
[2] M. Loosemore, A. Dainty, H. Lingard, Human Resource Management in Construction Projects: Strategic and Operational Approaches, Spon Press, London, United Kingdom, 2003 (ISBN: 978-0415261630).
[3] J.S. Petersen, C. Zwerling, Comparison of health outcomes among older construction and blue-collar employees in the United States, Am. J. Ind. Med. 34 (1998) 280–287 (doi: https://doi.org/10.1002/(SICI)1097-0274(199809)34:3 < 280::AID-AJIM11 > 3.0.CO;2-Q).
[4] J. Xiang, P. Bi, D. Pisaniello, A. Hansen, Health impacts of workplace heat exposure: an epidemiological review, Ind. Health 52 (2014) 91–101, http://dx.doi.org/10.2486/indhealth.2012-0145.
[5] O.O. Abbe, C.M. Harvey, L.H. Ikuma, F. Aghazadeh, Modeling the relationship between occupational stressors, psychosocial/physical symptoms and injuries in the construction industry, Int. J. Ind. Ergon. 41 (2011) 106–117, http://dx.doi.org/10.1016/j.ergon.2010.12.002.
[6] M.Y. Leung, Y.S. Chan, P. Olomolaiye, Impact of stress on the performance of construction project managers, J. Constr. Eng. Manag. 134 (2008) 644–652 (https://doi.org/10.1061/(ASCE)0733-9364(2008)134:8(644)).
[7] M.Y. Leung, Q. Liang, P. Olomolaiye, Impact of job stressors and stress on the safety behavior and accidents of construction workers, J. Manag. Eng. 32 (2015) 04015019 (https://doi.org/10.1061/(ASCE)ME.1943-5479.0000373).
[8] M. Loosemore, T. Waters, Gender differences in occupational stress among professionals in the construction industry, J. Manag. Eng. 20 (2004) 126–132 (https://doi.org/10.1061/(ASCE)0742-597X(2004)20:3(126)).
[9] F. Campbell, Occupational Stress in the Construction Industry, Chartered Institute of Building, Berkshire, UK, 2006https://www.census.gov/construction/c30/c30index.html , Accessed date: 14 April 2018.
[10] E. Jovanov, A.O. Lords, D. Raskovic, P.G. Cox, R. Adhami, F. Andrasik, Stress monitoring using a distributed wireless intelligent sensor system, IEEE Eng. Med. Biol. Mag. 22 (2003) 49–55, http://dx.doi.org/10.1109/MEMB.2003.1213626.
[11] D. Szafir, R. Signorile, An exploration of the utilization of electroencephalography and neural nets to control robots, Proceedings of the 13th IFIP TC 13 International Conference on Human-Computer Interaction, Springer-Verlag, New York City, NY, 2011, pp. 186–194, , http://dx.doi.org/10.1007/978-3-642-23768-3_16.
[12] J. Chen, B. Ren, X. Song, X. Luo, Revealing the “Invisible Gorilla” in construction: assessing mental workload through time-frequency analysis, 32nd International Symposium on Automation and Robotics in Construction and Mining (ISARC 2015), International Association for Automation & Robotics in Construction (IAARC), Oulu, Finland, 2015, http://dx.doi.org/10.22260/ISARC2015/0104.
[13] S.A. Hosseini, M.A. Khalilzadeh, Emotional stress recognition system using EEG and psychophysiological signals: using new labelling process of EEG signals in emotional stress state, 2010 International Conference on Biomedical Engineering and Computer Science (ICBECS), IEEE, Piscataway, New Jersey, 2010, pp. 1–6, , http://dx.doi.org/10.1109/ICBECS.2010.5462520.
[14] X. Hou, Y. Liu, O. Sourina, Y.R.E. Tan, L. Wang, W. Mueller-Wittig, EEG based stress monitoring, Systems, Man, and Cybernetics (SMC), IEEE, Kowloon, China, 2015, pp. 3110–3115, , http://dx.doi.org/10.1109/SMC.2015.540.
[15] R. Larson, M. Csikszentmihalyi, The experience sampling method, Flow and the Foundations of Positive Psychology, Springer, Dordrecht, 1983, , http://dx.doi.org/10.1007/978-94-017-9088-8_2.
[16] J. Chen, J.E. Taylor, S. Comu, Assessing task mental workload in construction projects: a novel electroencephalography approach, J. Constr. Eng. Manag. 143 (2017) 04017053 (https://doi.org/10.1061/(ASCE)CO.1943-7862.0001345).
[17] H. Jebelli, S. Hwang, S. Lee, Feasibility of field measurement of construction workers' valence using a Wearable EEG device, Computing in Civil Engineering 2017, ASCE, Reston, VA, 2017, pp. 99–106, , http://dx.doi.org/10.1061/9780784480830.013.
[18] D. Wang, J. Chen, D. Zhao, F. Dai, C. Zheng, X. Wu, Monitoring workers' attention and vigilance in construction activities through a wireless and wearable electroencephalography system, Autom. Constr. (2017), http://dx.doi.org/10.1016/j.autcon.2017.02.001.
[19] H. Jebelli, M.M. Khalili, S. Hwang, S. Lee, A supervised learning-based construction workers' stress recognition using a wearable Electroencephalography (EEG) Device, Construction Research Congress 2018, ASCE, Reston, VA, 2018, , http://dx.doi.org/10.1061/9780784481288.005.
[20] H. Jebelli, B. Choi, H. Kim, S. Lee, Feasibility study of a wristband-type wearable sensor to understand construction workers' physical and mental status, in: Construction Research Congress 2018, ASCE, Reston, VA, n.d. doi: https://doi.org/10.1061/9780784481264.036.
[21] H. Jebelli, S. Hwang, S. Lee, EEG signal-processing framework to obtain high-quality brain waves from an off-the-shelf wearable EEG device, J. Comput. Civ. Eng. 32 (2017) 04017070 (https://doi.org/10.1061/(ASCE)CP.1943-5487.0000719).
[22] S. Cohen, R.C. Kessler, L.U. Gordon, Measuring Stress: A Guide for Health and Social Scientists, Oxford University Press, Oxford, United Kingdom, 1997 (ISBN: 978-0195121209).
[23] L. Aftanas, N. Reva, A. Varlamov, S. Pavlov, V. Makhnev, Analysis of evoked EEG synchronization and desynchronization in conditions of emotional activation in humans: temporal and topographic characteristics, Neurosci. Behav. Physiol. 34 (2004) 859–867, http://dx.doi.org/10.1007/s11055-005-0151-9.
[24] K.H. Kim, S.W. Bang, S.R. Kim, Emotion recognition system using short-term monitoring of physiological signals, Med. Biol. Eng. Comput. 42 (2004) 419–427, http://dx.doi.org/10.1007/BF02344719.
[25] K. Takahashi, Remarks on emotion recognition from multi-modal bio-potential signals, International Conference on Industrial Technology (ICIT), IEEE, 2004, pp. 1138–1143, , http://dx.doi.org/10.1109/ICIT.2004.1490720.
[26] M. Sani, H. Norhazman, H. Omar, N. Zaini, S. Ghani, Support vector machine for classification of stress subjects using EEG signals, Systems, Process and Control (ICSPC), IEEE, 2014, pp. 127–131, , http://dx.doi.org/10.1109/SPC.2014.7086243.
[27] G. Jun, K. Smitha, EEG based stress level identification, Systems, Man, and Cybernetics (SMC), IEEE, 2016, pp. 003270–003274, , http://dx.doi.org/10.1109/SMC.2016.7844738.
[28] J.A. Urigüen, B. Garcia-Zapirain, EEG artifact removal-state-of-the-art and guidelines, J. Neural Eng. 12 (2015) 031001, http://dx.doi.org/10.1088/1741-2560/12/3/031001.
[29] T.C. Ferree, P. Luu, G.S. Russell, D.M. Tucker, Scalp electrode impedance, infection risk, and EEG data quality, Clin. Neurophysiol. 112 (2001) 536–544 (https://doi.org/10.1016/S1388-2457(00)00533-2).
[30] T. Jung, S. Makeig, C. Humphries, T. Lee, M.J. Mckeown, V. Iragui, T.J. Sejnowski, Removing electroencephalographic artifacts by blind source separation, Psychophysiology 37 (2000) 163–178, http://dx.doi.org/10.1111/1469-8986.3720163.
[31] S. Makeig, A.J. Bell, T.-P. Jung, T.J. Sejnowski, Independent component analysis of electroencephalographic data, Adv. Neural Inf. Proces. Syst. (1996) 145–151 https://papers.nips.cc/book/advances-in-neural-information-processing-systems-8-1995 (accessed April 14, 2018).
[32] A.G. Reddy, S. Narava, Artifact removal from EEG signals, Int. J. Comput. Appl. 77 (2013) 17–19, http://dx.doi.org/10.1088/1742-6596/90/1/012081.
[33] R.N. Vigário, Extraction of ocular artefacts from EEG using independent component analysis, Electroencephalogr. Clin. Neurophysiol. 103 (1997) 395–404, http://dx.doi.org/10.1016/S0013-4694(97)00042-8.
[34] L. Zhukov, D. Weinstein, C. Johnson, Independent component analysis for EEG source localization, IEEE Eng. Med. Biol. Mag. 19 (2000) 87–96, http://dx.doi.org/10.1109/51.844386.
[35] A. Delorme, S. Makeig, EEGLAB: an open source toolbox for analysis of single-trial EEG dynamics including independent component analysis, J. Neurosci. Methods 134 (2004) 9–21, http://dx.doi.org/10.1016/j.jneumeth.2003.10.009.
[36] M. Dash, H. Liu, Feature selection for classification, Intelligent Data Analy. 1 (1997) 131–156, http://dx.doi.org/10.1016/S1088-467X(97)00008-5.
[37] M. Hall, D.J. Buysse, P.D. Nowell, E.A. Nofzinger, P. Houck, C.F. Reynolds III, D.J. Kupfer, Symptoms of stress and depression as correlates of sleep in primary insomnia, Psychosom. Med. 62 (2000) 227–230, http://dx.doi.org/10.1097/00006842-200003000-00014.
[38] I. Guyon, A. Elisseeff, An introduction to variable and feature selection, J. Mach. Learn. Res. 3 (2003) 1157–1182 http://www.jmlr.org/papers/v3/guyon03a.html (accessed April 14, 2018).
[39] H. Candra, M. Yuwono, R. Chai, A. Handojoseno, I. Elamvazuthi, H.T. Nguyen, S. Su, Investigation of window size in classification of EEG-emotion signal with wavelet entropy and support vector machine, Engineering in Medicine and Biology Society (EMBC), IEEE, Milan, Italy, 2015, pp. 7250–7253, , http://dx.doi.org/10.

1109/EMBC.2015.7320065.
[40] N.S. Altman, An introduction to kernel and nearest-neighbor nonparametric regression, Am. Stat. 46 (1992) 175–185, http://dx.doi.org/10.2307/2685209.
[41] W. Daelemans, A. Van den Bosch, Memory-based Language Processing, Cambridge University Press, Cambridge, United Kingdom, 2005, http://dx.doi.org/10.1017/CBO9780511486579.
[42] K. Beyer, J. Goldstein, R. Ramakrishnan, U. Shaft, When is "Nearest Neighbor" meaningful? International Conference on Database Theory, Springer, Berlin, Heidelberg, 1999, pp. 217–235, , http://dx.doi.org/10.1007/3-540-49257-7_15.
[43] C.J. Burges, A tutorial on support vector machines for pattern recognition, Data Min. Knowl. Disc. 2 (1998) 121–167, http://dx.doi.org/10.1023/A:1009715923555.
[44] C. Liu, P. Rani, N. Sarkar, An empirical study of machine learning techniques for affect recognition in human-robot interaction, International Conference on Intelligent Robots and Systems, IEEE, Edmonton, Alta., Canada, 2005, pp. 2662–2667, , http://dx.doi.org/10.1109/IROS.2005.1545344.
[45] S. Hwang, H. Jebelli, B. Choi, M. Choi, S. Lee, Wearable EEG-based workers' emotional state measurement during construction task, J. Constr. Eng. Manag. 144 (2018) 04018050, , http://dx.doi.org/10.1061/(ASCE)CO.1943-7862.0001506.
[46] B.G. Berger, Psychological benefits of an active lifestyle: what we know and what we need to know, Quest 48 (1996) 330–353, http://dx.doi.org/10.1080/00336297.1996.10484201.
[47] M.Y. Leung, Q. Liang, I.Y. Chan, Development of a stressors–stress–performance–outcome model for expatriate construction professionals, J. Constr. Eng. Manag. (2016) 04016121, , http://dx.doi.org/10.1061/(ASCE)CO.1943-7862.0001266.
[48] K. Mignonac, O. Herrbach, Linking work events, affective states, and attitudes: an empirical study of managers' emotions, J. Bus. Psychol. 19 (2004) 221–240, http://dx.doi.org/10.1007/s10869-004-0549-3.
[49] A. Levine, O. Zagoory-Sharon, R. Feldman, J.G. Lewis, A. Weller, Measuring cortisol in human psychobiological studies, Physiol. Behav. 90 (2007) 43–53, http://dx.doi.org/10.1016/j.physbeh.2006.08.025.
[50] F. Al-Shargie, T.B. Tang, M. Kiguchi, Assessment of mental stress effects on prefrontal cortical activities using canonical correlation analysis: an fNIRS-EEG study, Biomed. Opt. Express. 8 (2017) 2583–2598, http://dx.doi.org/10.1364/BOE.8.002583.
[51] F. Al-shargie, T.B. Tang, N. Badruddin, M. Kiguchi, Mental stress quantification using EEG signals, International Conference for Innovation in Biomedical Engineering and Life Sciences, Springer, 2015, pp. 15–19, , http://dx.doi.org/10.1007/978-981-10-0266-3_4.
[52] X. Jie, R. Cao, L. Li, Emotion recognition based on the sample entropy of EEG, Biomed. Mater. Eng. 24 (2014) 1185–1192, http://dx.doi.org/10.3233/BME-130919.
[53] K.-Q. Shen, C.-J. Ong, X.-P. Li, Z. Hui, E.P. Wilder-Smith, A feature selection method for multilevel mental fatigue EEG classification, IEEE Trans. Biomed. Eng. 54 (2007) 1231–1237, http://dx.doi.org/10.1109/TBME.2007.890733.
[54] G.C. Cawley, N.L. Talbot, On over-fitting in model selection and subsequent selection bias in performance evaluation, J. Mach. Learn. Res. 11 (2010) 2079–2107 http://www.jmlr.org/papers/v11/cawley10a.html (accessed April 14, 2018).
[55] C.-W. Hsu, C.-J. Lin, A comparison of methods for multiclass support vector machines, IEEE Trans. Neural Netw. 13 (2002) 415–425, http://dx.doi.org/10.1109/72.991427.